



Disilane- and siloxane-bridged biphenyl and bithiophene derivatives as electron-transporting materials in OLEDs

Hiroyuki Kai^a, Joji Ohshita^{a,*}, Sayaka Ohara^a, Naohiro Nakayama^a, Atsutaka Kunai^a, In-Sook Lee^b, Young-Woo Kwak^b

^a Department of Applied Chemistry, Graduate School of Engineering, Hiroshima University, Higashi-Hiroshima 739-8527, Japan

^b Department of Chemistry, Kyungpook National University, Daegu 702-701, South Korea

ARTICLE INFO

Article history:

Received 22 April 2008

Received in revised form 5 August 2008

Accepted 18 August 2008

Available online 22 August 2008

Keywords:

Silole

OLED

Electron-transport

Theoretical calculation

ABSTRACT

Optical, electrochemical, and electron-transporting properties of disilane- and siloxane-bridged biphenyl and bithiophene derivatives were investigated, in comparison with those of the monosilane-bridged analogues (siloles). The UV spectra and cyclic voltammograms indicated that elongation of the silicon bridge suppresses the π -conjugation, in accordance with the results of DFT calculations. The DFT calculations indicated also that the disilane-bridged biphenyl and siloxane-bridged bithiophene should have the low-lying HOMOs and LUMOs. The electron-transporting properties were evaluated by the performance of triple-layered OLEDs having vapor-deposited films of the Si-bridged compound, Alq₃, and TPD, as the electron-transport, emitter, and hole-transport, respectively. Of these, the device with a disilane-bridged biphenyl exhibited the high performance with the maximum current density of 590 mA/cm² at the applied electric field of 12×10^7 V/m (applied bias voltage = 13 V) and the maximum luminance of 22 000 cd/m² at 13×10^7 V/m.

© 2008 Elsevier B.V. All rights reserved.

1. Introduction

Much attention has been focused on the silole ring system, in which the σ^* -orbital of the silicon atom effectively interacts with the π^* -orbital of the butadiene unit, leading to the low-lying LUMO [1]. To date, many papers concerning the functionalities of silole-based materials have been published [2], since a bipyridyl-substituted silole has been demonstrated to be usable as an efficient electron-transporting material in multi-layered organic light-emitting diodes (OLEDs) [3,4].

Annulated silole derivatives, such as dibenzosiloles (Chart 1, 1), have been also studied as OLED materials. Fascinating properties of dibenzosilole–fluorene copolymers have been reported. For example, incorporation of dibenzosilole units into the π -conjugated polyfluorene main chain leads to high-efficiency spectrum-stable color-pure blue-emitting materials [5]. We have studied dithienosilole as a thiophene-annulated silole system (Chart 1, 4) and have demonstrated that dithienosilole derivatives also exhibit highly electron-transporting properties in their vapor-deposited films, being applicable to OLEDs [6,7]. Disilane-bridged bithiophenes (Chart 1, 5) again can be used as excellent electron-transporters in OLEDs, similar to dithienosiloles [7]. Recently we have studied the optical, and electrochemical properties of a siloxane-bridged

bithiophene (Chart 1, 6) and it has been demonstrated that introducing an oxygen atom into the disilane unit affects primarily the HOMO energy level to lower it, with the LUMO level being almost untouched. This clearly indicates that the siloxane-bridged bithiophene can be anticipated as efficient electron-transporting materials with good hole-blocking properties [8]. However, the electron-transporting properties have not yet been examined.

In this paper, we discuss the results of theoretical calculations on simplified model compounds that have disilane- and siloxane-bridged biphenyl and bithiophene units (Chart 1), and the optical and electrochemical properties of these compounds, in comparison with those of dibenzo- and dithienosiloles. Performance of triple-layered OLEDs having vapor-deposited films of these compounds as the electron-transporting materials is also described.

2. Results and discussion

2.1. Theoretical calculations on Si-bridged biphenyls and bithiophenes

The relative HOMO and LUMO energy levels for the model compounds **1a–5a** derived from DFT [9,10] calculations are depicted in Fig. 1. As can be seen in Fig. 1, the LUMO energy level of disilane-bridged biphenyl **2a** is comparable to that of dibenzosilole **1a**, while HOMO of **2a** lies at lower level than that of **1a** by 0.20 eV. On the other hand, the LUMO level of **3a** is considerably affected by introducing an oxygen atom, elevating the level by 0.32 eV from

* Corresponding author.

E-mail address: jo@hiroshima-u.ac.jp (J. Ohshita).

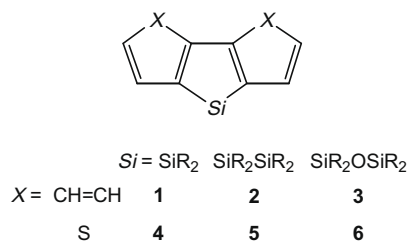


Chart 1. Si-bridged biphenyl and bithiophene derivatives.

that of **2a**. For the LUMOs, two factors seem to be operative in these compounds, one of which is the twisting of two benzene rings, and the other is the degree of $\sigma^*-\pi^*$ conjugation. Compound **2a** possesses a twisted biphenyl unit with the dihedral angle of $\text{C}=\text{C}-\text{C}=\text{C} = 42.1$ deg, as shown in Fig. 1, suppressing the π -conjugation between the benzene units. This may be roughly balanced with the enhanced $\sigma^*-\pi^*$ conjugation in disilane **2a**, resulting in the LUMO energy level, similar to that of monosilane **1a**. For **3a**, the $\sigma^*-\pi^*$ conjugation is interrupted by the oxygen atom and the twisting is much more enhanced.

For bithiophene derivatives, the HOMO energy levels were calculated to be higher than those of biphenyl derivatives, probably due to the electron-donating properties of thiophene rings. Introduction of an oxygen atom to **5a** giving rise to **6a** exerts little influence on the LUMO energy level, in contrast to that the LUMO of **3a** is at higher energy than that of **2a**. In **6a**, the electronegative oxygen appears to lower the LUMO by its inductive effect, which may compensate the reduced $\sigma^*-\pi^*$ conjugation. Thiophene ring system, which is essentially electron-donating, would be more affected by the inductive effect of the oxygen inserted, as compared with benzene system. Similarly, the HOMO of **6a** is much more influenced by the oxygen to lower the energy level significantly, as compared with **3a**. The smaller twisting of the bithiophene unit in **6a** ($\text{C}=\text{C}-\text{C}=\text{C} = 38.7$ deg) than that in **3a** ($\text{C}=\text{C}-\text{C}=\text{C} = 54.1$ deg) seems to be primarily responsible for smaller HOMO–LUMO energy gap for **6a**.

It is noteworthy that the LUMOs of **2a**, and **6a** lay at the energies, approximately as low as that of **5a**, while they have the

HOMOs at much lower levels than **5a**. Disilane-bridged bithiophene **5** has proven to work as an excellent electron-transport in OLEDs [7], and hence we expected compounds **2** and **6** as electron-transporters with better electron-blocking than **5**. We also examined dibenzosilole (**1**) as the electron-transport, since nothing has been reported for electron-transporting properties of monomeric dibenzosiloles, to our knowledge.

2.2. Synthesis of disilane- and siloxane-bridged biphenyls **2b**, **2c**, and **3b**

Si-bridged biphenyls **2b**, **2c**, and **3b** were synthesized as shown in Scheme 1. Compound **2b** was obtained by an in-situ Grignard reaction of dibromobiphenyl and the dichlorodimethyldiphenyldisilane with magnesium in 51% yield as a colorless solid composed of 1:4 cis and trans isomers. A similar reaction with dichlorotetraethylsilane afforded compound **2c** in 32% yield as a colorless oil. Treatment of disilane-bridged biphenyl (**2d**) with trimethylamine oxide produced siloxane **3b**.

2.3. Optical and electrochemical properties of Si-bridged biphenyls and bithiophenes

Table 1 summarizes the UV absorption maxima and oxidation peak potentials in the cyclic voltammograms (CVs) of Si-bridged biphenyls and bithiophenes (see Scheme 1 and Chart 2). The UV absorption maxima moved to longer wave length in the order of **3b** < **2b,c** < **1b** < **6b** < **5b** in accordance with the results of DFT calculations.

The CVs of the present Si-bridged biphenyls and bithiophenes were measured in acetonitrile. These compounds underwent irreversible oxidation in CVs without reductive counter waves, indicating some decompositions such as polymerization occurred during the measurements. The oxidation peak potentials were noted as listed in Table 1, which moved to lower potentials, in the order of **3b** > **1b** > **2b,c**, **6b** > **5b**. This is in accordance with the results of DFT calculations, which indicate the HOMO energy levels are elevated in the same order, except for **1b**. The reason for higher oxidation potential for **1b** than that expected from the calculations is not clear yet. However, the irreversible CV profiles for these com-

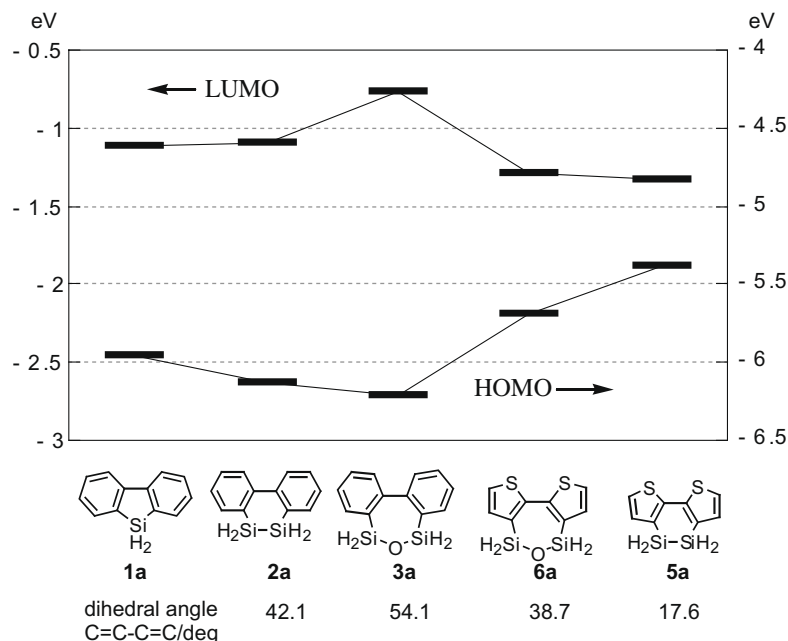
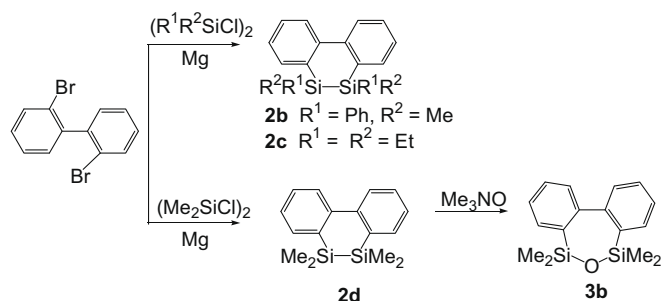


Fig. 1. Relative HOMO and LUMO energy levels of Si-bridged biphenyl and bithiophene derivatives based on DFT calculations at the level of B3LYP/6-31G(d,p).



Scheme 1.

Table 1
Properties of Si-bridged biphenyls and bithiophenes

Compound	Absorption ^a λ_{\max} /nm	CV ^b E_{pa}/V^c
1b	320	1.4
2b	290	1.1
2c	281	1.0
3b	243	1.9
5b^d	350	0.8
6b^e	324	1.0

^a In THF or CHCl_3 .

^b In acetonitrile containing 100 mM LiClO_4 as the supporting electrolyte using Pt plates as the working and counter electrodes.

^c Anodic peak potential versus Ag/Ag^+ .

^d Data taken from Ref. [7].

^e Data taken from Ref. [8].

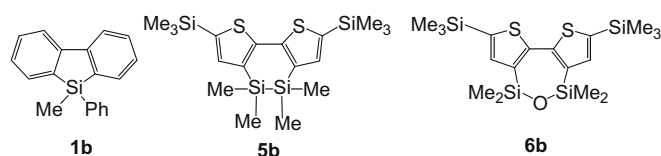


Chart 2.

pounds would not allow us to discuss the electronic states of the compounds in detail on the basis of the oxidation peak potentials.

2.4. OLED performance of the devices having **2b** and **6b** as the electron-transport

To evaluate electron-transporting properties of the present Si-bridged biphenyl and bithiophene, we fabricated triple-layered OLEDs having a vapor-deposited layer of **2b** or **6b** as the electron-transport. The structure of the devices and the thickness of the layers were ITO/TPD (40 nm)/ Alq_3 (50 nm)/**2b** or **6b** (20 nm)/Mg–Ag (device A for **2b** and device B for **6b**) where Alq_3 and TPD were tris(8-quinolinolato)aluminium (III) and *N,N'*-diphenyl-*N,N'*-di-*m*-tolylbiphenyl-4,4'-diamine, respectively. In these devices, TPD, **2b** or **6b**, and Alq_3 layers were the hole- and electron-transport, and the emitter, and ITO and Mg–Ag were the anode and cathode, respectively. We also examined device C having a layer of **1b** as the electron-transport in place of **2b/6b** (ITO/TPD (40 nm)/ Alq_3 (50 nm)/**1b** (20 nm)/Mg–Ag), and a typical double-layered device D without the electron-transport layer (ITO/TPD (40 nm)/ Alq_3 (50 nm)/Mg–Ag). One might consider that the LUMOs of **2b** and **6b** would be at higher level than Alq_3 (–2.59 eV [11]). For example, the LUMO energy level for **6b** from the onset of CV oxidation and UV absorption edge was estimated to be –2.2 eV [12]. However, it is not unusual to assume that the electronic states may strongly depend on the conditions, in solutions or films. In

condensed films, stacking of the molecules would considerably affect the electronic states. In fact, the UV spectrum of a vapor-deposited film of compound **2b** showed shoulders around 300 and 320 nm, together with the absorption maximum at almost the same energy as that in a solution (280 nm). Moreover, emission spectrum of **2b** in THF showed a band at 355 nm, but the band disappeared for its vapor-deposited film. These results are indicative of intermolecular interaction between chromophores in the condensed phase. We could not estimate the LUMO level of **2b**, due to its broad oxidation peak.

By applying the electric field, these devices emitted green light arising from Alq_3 emission. Fig. 2 depicts the current density–electric field (*I*–*V*) characteristics of the devices, indicating that device A with **2b** exhibited the best *I*–*V* characteristics among the devices examined. Device A showed the maximum current density of 590 mA/cm² at the electric field of 12×10^7 V/m (applied bias voltage = 13 V). That all three triple-layered devices A–C showed higher current density in whole region of the electric field than device D indicates the electron-transporting properties of the vapor-deposited films of **1b**, **2b**, and **6b**. The luminance–electric field (*L*–*V*) characteristics of the devices are presented in Fig. 3. The maximum luminance from device A was as high as 22000 cd/m² at 13×10^7 V/m. Despite our expectation based on the DFT calculations, luminance of device B with **6b** was much lower than that of devices C and D in the whole region of the applied electric field, with the maximum luminance of 1530 cd/m² at 11×10^7 V/m. Since device B showed the *I*–*V* characteristics, a little inferior but comparable to those of A, the low luminance seems to be due to the insufficient hole-blocking properties of the layer of **6b**.

In conclusion, we studied novel Si-bridged biphenyl and bithiophene derivatives that were predicted to possess low-lying HOMO and LUMO by DFT calculations. OLEDs having vapor-deposited films of these compounds as the electron-transport, were fabricated and their performance was examined. Excellent device performance was demonstrated for the OLED with disilane-bridged biphenyl **2b**. It was also found that the siloxane-bridged bithiophene was potentially useful as an electron-transporting material.

3. Experimental

3.1. General

All reactions were carried out under an inert atmosphere. NMR spectra were recorded on JEOL Model JNM-EX 270 and JEOL Model JNM-LA 400 spectrometers. Mass spectra were measured with a Hitachi M80B spectrometer. UV spectra were measured on a Hitachi U-3210 spectrophotometer. The usual workup mentioned in the following part involves separating the organic layer, extracting the aqueous layer, drying the combined organic layer and the extracts, and evaporating the solvents, in that order.

3.2. Materials

THF and toluene were dried over sodium and distilled just before use. Acetonitrile was distilled from P_2O_5 and stored in dark under an argon atmosphere at 4 °C before use.

3.3. Preparation of **2b,c**

In a 30 mL three-necked flask fitted with a dropping funnel were placed 0.17 g (6.9 mol) of magnesium, 1,2-dichloro-1,2-dimethyl-1,2-diphenyldisilane (1.0 g 3.2 mol), and 5 mL of THF. To this was added a solution of 2,2'-dibromobiphenyl (1.0 g 3.2 mol) in 20 mL of THF at room temperature. The resulting mixture was refluxed for 30 min. The mixture was then cooled to room temper-

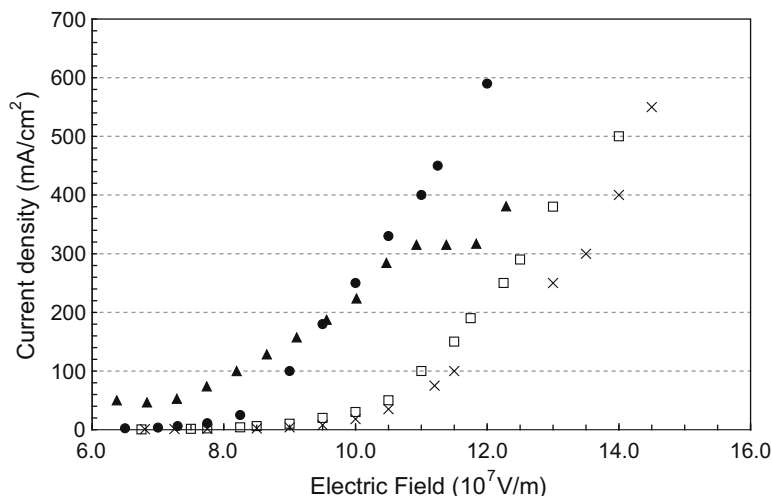


Fig. 2. Plots of operating electric field vs current density of (●) device A, (▲) device B, (□) device C (×) device D.

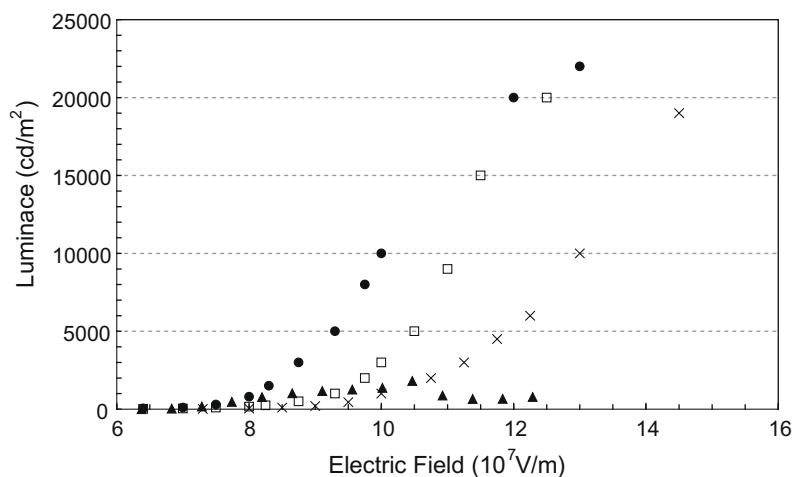


Fig. 3. Plots of operating electric field vs luminance of (●) device A, (▲) device B, (□) device C (×) device D.

ature and was hydrolyzed with water. After the usual workup, the residue was chromatographed on a silica gel column with hexane/ethyl acetate (10/1 vol%) as eluent to give **2b** as a 1:4 cis/trans isomeric mixture (yield 51%), which was recrystallized from ethanol to give **2b** as a colorless solid (yield 9%): m.p. 84.5–89.0 °C; MS m/z 392 (M^+); 1H NMR (δ in $CDCl_3$) 0.45 (s, 6H, Me), 7.07–7.28 (m, 14H, ring protons), 7.37 (t, 2H, $J = 7.5$ Hz, ring protons), 7.45 (d, 2H, $J = 7.5$ Hz, ring protons). Anal. Calc. for $C_{26}H_{24}Si_3$: C, 79.53; H, 6.16. Found: C, 79.33; H, 6.19%.

Compound **2c** was prepared in a fashion similar to **2b**, using 1,2-dichloro-1,1,2,2-tetraethylidisilane instead of 1,2-dichloro-1,2-dimethyl-1,2-diphenyldisilane. Data for **2c**: 32% yield; colorless oil; MS m/z 324 (M^+); 1H NMR (δ in $CDCl_3$) 0.81 (q, 8H, $J = 7.0$ Hz, CH_2CH_3), 0.92 (t, 12H, $J = 7.0$ Hz, CH_2CH_3), 7.23–7.28 (m, 2H, phenyl ring protons), 7.40–7.42 (m, 4H, ring protons), 7.45 (dd, 2H, $J = 7.01$ Hz, $J = 1.09$ Hz, ring protons); ^{13}C NMR (δ in $CDCl_3$) 3.18, 8.73 (Et), 126.33, 129.76, 129.93, 133.68, 134.05, 148.10 (ring carbons). Anal. Calc. for $C_{20}H_{28}Si_2$: C, 74.00, H, 8.96. Found: C, 74.02; H, 6.76%.

3.4. Preparation of **3b** [13]

In a 50 mL three-necked flask fitted with a reflux condenser was placed a mixture of 0.20 g (0.75 mmol) of **2d** that was prepared in a fashion similar to **2b**, using 1,2-dichloro-1,1,2,2-tetramethyldisilane

instead of 1,2-dichloro-1,2-dimethyl-1,2-diphenyldisilane, and 0.17 g (2.24 mol) of trimethylamine oxide in 30 mL of dry toluene. After being stirred at room temperature for 2 day, the mixture was hydrolyzed with water. After the usual workup, the residue was chromatographed on a GPC column with toluene as eluent to give **3b** (yield 42%) as a colorless solid: mp 74.9 °C (DSC); MS m/z 284 (M^+); 1H NMR (δ in $CDCl_3$) –0.28 (s, 6H, MeSi), 0.55 (s, 6H, MeSi), 7.38–7.56 (m, 6H, ring protons), 7.63 (d, 2H, $J = 7.6$ Hz, ring protons); ^{13}C NMR (δ in $CDCl_3$) –0.64, 0.13 (Me), 126.47, 130.06, 133.03, 137.99, 149.44 (ring carbons). Anal. Calc. for $C_{16}H_{20}Si_2O$: C, 67.55; H, 7.09. Found: C, 67.09; H, 7.29%.

3.5. DFT calculations

The density functional theory (DFT) calculations were carried out using the Gaussian03 program package [10]. The Becke-three-parameter-Lee–Yang–Parr hybrid functional [14–17] was employed with the 6-31G(d,p) basis set.

3.6. CV measurements

CV measurements were carried out using a three-electrode system in acetonitrile solutions containing 100 mM of lithium perchlorate as the supporting electrolyte and 2 mM of the substrate. Pt wires were used as the working and counter electrodes, and

Ag/Ag⁺ was used as the reference electrode. The current-electric field curves were recorded at room temperature on a Hokuto Denko HAB-151 potentiostat/galvanostat.

3.7. Preparation of OLEDs

Each layer of the OLEDs was prepared by vacuum deposition at 1×10^{-5} torr in the order of TPD, Alq₃, and the present compound, on ITO coated on a glass substrate with a sheet resistance of 15 Ω/cm (Nippon Sheet Glass Company). Finally a layer of magnesium-silver alloy with an atomic ratio of 10:1 was vacuum deposited as the top electrode. The emitting area was 5×5 mm².

Acknowledgments

This work was supported by a Grant-in-Aid for Science Research (No. 20350092) from the Ministry of Education, Culture, Sports, Science and Technology, Japan.

References

- [1] (a) S. Yamaguchi, K. Tamao, Chem. Lett 34 (2005) 2;
(b) S. Yamaguchi, K. Tamao, J. Chem. Soc., Dalton Trans (1998) 3693.
- [2] (a) K. Tamao, S. Yamaguchi, M. Shiozaki, Y. Nakagawa, Y. Ito, J. Am. Chem. Soc. 114 (1992) 5867;
(b) G. Zhang, J. Ma, Y. Jiang, Macromolecules 36 (2003) 2130;
(c) J. Lee, Q.-D. Liu, M. Motola, J. Dane, J. Gao, Y. Kang, S. Wang, Chem. Mater. 16 (2004) 1869;
(d) G. Yu, S. Yin, Y. Liu, J. Chen, X. Xu, X. Sun, D. Ma, X. Zhan, Q. Peng, Z. Shuai, B. Tang, D. Zhu, W. Fang, Y. Luo, J. Am. Chem. Soc. 127 (2005) 6335;
(e) X. Zhan, C. Risko, F. Amy, C. Chan, W. Zhao, S. Barlow, A. Kahn, J.-L. Brédas, S. Marder, J. Am. Chem. Soc. 127 (2005) 9021;
(f) K. Geramita, J. McBee, Y. Shen, N. Radu, T.D. Tilley, Chem. Mater. 18 (2006) 3261;
(g) J. Lee, Y.-Y. Yuan, Y. Kang, W.-L. Jia, Z.-H. Lu, S. Wang, Adv. Funct. Mater. 16 (2006) 681;
(h) H.-J. Son, W.-S. Han, J.-Y. Chun, C.-J. Lee, J.-I. Han, J. Ko, S.O. Kang, Organometallics 26 (2007) 519.
- [3] (a) M. Uchida, T. Izumikawa, T. Nakano, S. Yamaguchi, K. Tamao, Chem. Mater. 13 (2001) 2680;
(b) W. Kim, L.C. Palilis, M. Uchida, Z.H. Kafafi, Chem. Mater. 16 (2004) 4681.
- [4] K. Tamao, M. Uchida, T. Izumikawa, K. Furukawa, S. Yamaguchi, J. Am. Chem. Soc. 116 (1996) 11974.
- [5] E. Wang, C. Li, Y. Mo, Y. Zhang, G. Ma, W. Shi, J. Peng, P. Yang, Y. Cao, J. Mater. Chem. 16 (2006) 4133.
- [6] (a) J. Ohshita, H. Kai, A. Takata, T. Iida, A. Kunai, N. Ohta, K. Komaguchi, M. Shiotani, A. Adachi, K. Sakamaki, K. Okita, Organometallics 20 (2001) 4800;
(b) J. Ohshita, K. Kimura, K.-H. Lee, A. Kunai, Y.-W. Kwak, E.-C. Son, J. Polym. Sci., A: Polym. Chem 45 (2007) 4588;
(c) J. Ohshita, H. Kai, T. Sumida, A. Kunai, A. Adachi, K. Sakamaki, K. Okita, Organomet. Chem 642 (2002) 137.
- [7] J. Ohshita, M. Nodono, H. Kai, T. Watanabe, A. Kunai, K. Komaguchi, M. Shiotani, A. Adachi, K. Okita, Y. Harima, K. Yamashita, M. Ishikawa, Organometallics 18 (1999) 1453.
- [8] Y.-W. Kwak, I.-S. Lee, M.-K. Baek, U. Lee, H.-J. Choi, M. Ishikawa, A. Naka, J. Ohshita, K.-H. Lee, A. Kunai, Organometallics 25 (2006) 48.
- [9] Results of DFT-calculations, and electrochemical and optical properties of disilane- and siloxane-bridged bithiophene at a different level of the theory have been already reported, see Ref. [8].
- [10] M.J. Frisch, G.W. Trucks, H.B. Schlegel, G.E. Scuseria, M.A. Robb, J.R. Cheeseman, V.G. Zakrzewski, J.A. Montgomery Jr., R.E. Stratmann, J.C. Burant, S. Dapprich, J.M. Millam, A.D. Daniels, K.N. Kudin, M.C. Strain, O. Farkas, J. Tomasi, V. Barone, M. Cossi, R. Cammi, B. Mennucci, C. Pomelli, C. Adamo, S. Clifford, J. Ochterski, G.A. Petersson, P.Y. Ayala, Q. Cui, K. Morokuma, D.K. Maliek, A.D. Rabuck, K. Raghavachari, J.B. Foresman, J. Cioslowski, J.V. Ortiz, B.B. Stefanov, G. Liu, A. Liashenko, P. Piskorz, I. Komaromi, R. Gomperts, R.L. Martin, D.J. Fox, T. Keith, M.A. Al-Lalam, C.Y. Peng, A. Nanayakkara, C. Gonzalez, M. Challacombe, P.M.W. Gill, B.G. Johnson, W. Chen, M.W. Wong, J.L. Andres, M. Head-Gordon, E.S. Replogle, J.A. Pople, Program Packages from GAUSSIAN, Inc., Pittsburgh, PA.
- [11] J.D. Anderson, E.M. McDonald, P.A. Lee, M.L. Anderson, E.L. Ritchie, H.K. Hall, T. Hopkins, A. Padias, S. Thayumanavan, S. Barlow, S.R. Marder, G.E. Jabbour, S. Shaheen, B. Kippelen, N. Peyghambarian, R.M. Wightman, N.R. Armstrong, E.A. Mash, J. Wang, J. Am. Chem. Soc. 120 (1998) 9646.
- [12] The LUMO energy level of **2b** could not be estimated because of the broadness of the CV peak.
- [13] M. Kira, K. Sakamoto, H. Sakurai, J. Am. Chem. Soc. 105 (1963) 7469.
- [14] A.D. Becke, Phys. Rev. A 38 (1988) 3098.
- [15] C. Lee, W. Yang, R.G. Parr, Phys. Rev. B 37 (1988) 785.
- [16] A.D. Becke, J. Chem. Phys. 98 (1993) 1372.
- [17] P.M.W. Gill, B.G. Johnson, J.A. Pople, Int. J. Quantum Chem. Symp. 26 (1992) 319.